ELSEVIER Applied Mathematics and Computation 116 (2000) 197–215

APPLIED MATHEMATICS AND COMPUTATION

www.elsevier.com/locate/amc

The estimation of aerosol optical parameters from ADEOS/POLDER data

Yoshiyuki Kawata [a,*], Toshiaki Izumiya [a], Akihiro Yamazaki [b]

[a] *Environmental Information Research Lab, Kanazawa Institute of Technology, Ogigaoka 7-1, Nonoichi-machi Ishikawa, 921 Japan*

[b] *Meteorological Research Institute, Nagamine 1–1, Tsukuba 305-0052, Japan*

Abstract

A cross calibration analysis between POLDER and OCTS sensors on board ADEOS satellite in terms of the space reflectance was made. Space reflectance values, computed from the POLDER and OCTS data (acquired simultaneously on 26 April 1997) for the same ocean target, were examined and we found that they are in good agreement in all bands, when the new in-flight calibration gain factors for each sensor are assumed. Furthermore, we retrieved aerosol optical parameters (i.e., the optical thickness, Ångström exponent, and refractive index) by using several retrieving algorithms from using ADEOS/POLDER's directional space reflectance and polarization data in infrared bands simultaneously. Retrieved results were presented by the form of distribution maps. In addition, good and bad points of each retrieval algorithm were discussed. Finally, we proposed an improved method for retrieving aerosol optical parameters, which utilizes theoretical P–SR (polarization–space reflectance) diagrams at given viewing angles in an 865 nm band. The estimated aerosol optical parameters by our proposed method were compared with the simultaneously measured sky observation data. We found an excellent agreement between them.

Keywords: Aerosol optical parameters; Space reflectance; Polarization; Retrieval algorithm; POLDER

* Corresponding author.
E-mail address: kawata@infor.kanazawa-it.ac.jp (Y. Kawata).

0096-3003/00/$ - see front matter
PII: S0096-3003(99)00205-2

1. Introduction

CNES's POLDER sensor, on board NASDA's ADEOS satellite, had collected the global data sets for about eight months during the ADEOS's operational period (launched in August 1996 – ended in June 1997). Since the POLDER and OCTS are on the same ADEOS satellite and they have six nearly identical spectral bands, centered at 443, 490, 565, 670, 765, and 865 nm, it may be possible to make a cross calibration between two sensors. In the cross calibration analysis the latest information on the calibration coefficients for POLDER and OCTS after launch [1,2] were used. Furthermore, it may be possible to retrieve the aerosol optical parameters using ADEOS/POLDER's directional reflectance and polarization data simultaneously in the 865 nm band.

2. Theoretical background

The incident solar flux vector in Stokes vector representation is given by Eq. (1):

$$\pi\mathbf{F} = \pi[f\,0\,0\,0]^{\mathrm{t}}, \tag{1}$$

where a superscript represents the matrix transposition. In this notation we assume an incident solar flux vector $\pi\mathbf{F}$ illuminates a plane parallel atmosphere with the optical thickness of τ_{at} in the direction of (μ_0, ϕ_0) , where μ_0 and ϕ_0 are the cosine of solar zenith angle θ_0 and the solar azimuth angle ϕ_0, respectively. In the right side πf equals to the extraterrestrial irradiance per unit area normal to the direction of solar rays, E_{s} (W/m^2). Then, the upwelling Stokes vector at the top of the atmosphere (TOA) in the direction of (μ, ϕ), $\mathbf{I}(\tau_{\mathrm{at}}, \mu, \mu_0, \phi - \phi_0) = [I\,Q\,U\,V]^{\mathrm{t}}$ can be expressed by Eq. (2) in terms of the reflection matrix of the atmosphere–ocean system $\mathbf{R}_{\mathrm{at+sf}}$:

$$\mathbf{I}(\tau_{\mathrm{at}}, \mu, \mu_0, \phi - \phi_0) = \mu_0\mathbf{R}_{\mathrm{at+sf}}(\tau_{\mathrm{at}}, \mu, \mu_0, \phi - \phi_0)\mathbf{F}. \tag{2}$$

As for the components of Stokes vector, I is the radiance, Q related to the linear polarization, U to the plane of polarization, and V to the circular polarization. In the Earth's atmosphere the circular polarization can be ignored. By using the adding method [3], $\mathbf{R}_{\mathrm{at+sf}}$ can be expressed in terms of the reflection matrix, the transmission matrix of the atmosphere and the reflection matrix of the sea surface, $\mathbf{R}_{\mathrm{at}}, \mathbf{T}_{\mathrm{at}}$, and $\mathbf{R}_{\mathrm{sf}}$, respectively. For the basic formulations of these matrices for a single atmospheric layer with a Gaussian type ocean surface (Cox–Munk model [4]), refer to our previous paper [5].

The definitions of the space reflectance $\mathbf{R}_{\mathrm{sp}}$ at TOA and degree of linear polarization P in the reflected radiation are given by Eqs. (3) and (4), respectively:

$$R_{sp} = \pi I/\mu_0 E_s = \pi I/\mu_0(\pi f) = I/\mu_0, \tag{3}$$

$$P = \frac{\sqrt{Q^2 + U^2}}{I}. \tag{4}$$

For simplicity, we shall call it the polarization in this paper.

3. Cross calibration between POLDER and OCTS

We have made the cross calibration between POLDER and OCTS sensors, using the reflected radiance data acquired simultaneously on 26 April 1997. A target site (N37.5–N37.97; E142.0–E142.5) is shown by a parallelogram in both OCTS and POLDER images (Fig. 1). We divided the target area into 16 small blocks and computed the mean space reflectances for each blocked area from measured reflected radiances by POLDER and OCTS, using their in-flight calibration coefficients. In the computation we adopted the latest in-flight calibration gain factors for POLDER [1] and OCTS [2]. The observational angular conditions at the target center were rather different for POLDER and OCTS, because we selected the target site in scene 43 which seemed without the effect of specular reflection. The POLDER and OCTS cases were $(\theta_0 = 26.81,\ \theta = 35.86,\ \phi - \phi_0 = 159.59)$ and $(\theta_0 = 26.79,\ \theta = 21.95,\ \phi - \phi_0 = 212.08)$, respectively. We estimated the effects in all bands due to different angular conditions, by assuming a typical aerosol optical model with $(\tau_{500} = 0.2,\ \alpha = 1.5,\ m = 1.40 - i0.0)$, where τ_{500}, α, and m are the aerosol optical thickness at 500 nm, Ångström exponent, and the aerosol refractive index, respectively. The adoption of this aerosol model for the target site was

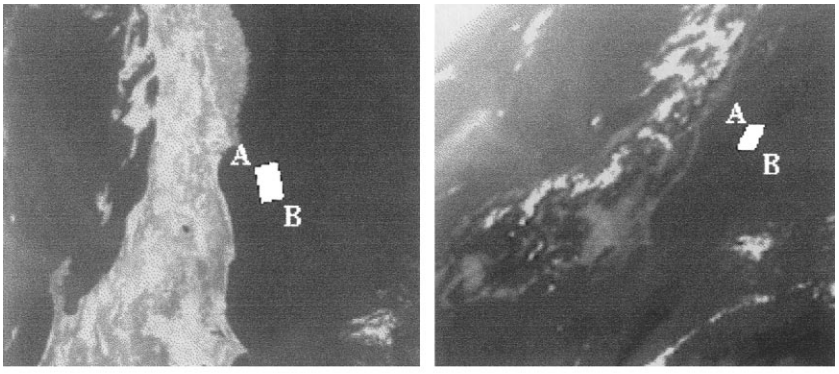

Fig. 1. Location of the target area: (a) image by OCTS; (b) scene 43 by POLDER.

Table 1
In-flight calibration and angular gain factors

λ (nm)	POLDER gain	OCTS gain	Angular gain
443	0.9700	1.0300	1.1231
490	0.9900	0.9394	1.1234
565	1.0350	1.0400	1.1140
670	1.0300	1.0000	1.1035
765	1.0350	1.0200	1.0868
865	1.0500	0.8900	1.0800

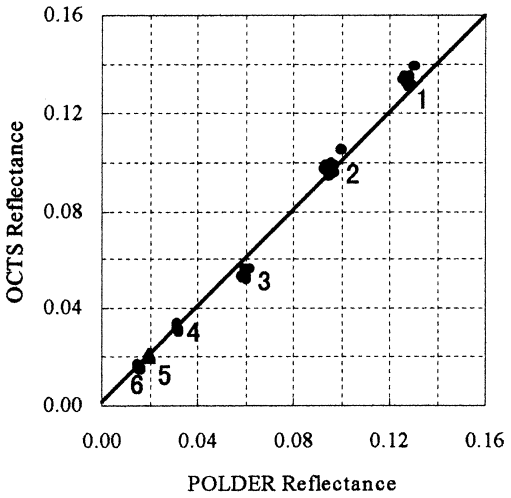

Fig. 2. Correlation in space reflectance between POLDER and OCTS. Spectral channel (band) numbers are in the figure.

based on the retrieved results by Method A with fixed refractive index of $m = 1.40 - i0.0$ (described in the next section). The in-flight gain factors for POLDER and OCTS are listed in Table 1, together with the angular gain factors for normalizing the angular condition of OCTS to that of POLDER. The computed mean space reflectances at the target site for the cases of POLDER and OCTS are shown in Fig. 2 and Table 2. Space reflectance between POLDER and OCTS is in good agreement with relative differences of less than 10% in all bands (channels).

4. Estimation of aerosol parameters

We investigated several methods for estimating aerosol optical parameters, using POLDER's directional reflectance and polarization data at 670 and

Table 2
Space reflectances of ocean target by POLDER and OCTS and their relative differences

Ch.	λ (nm)	POLDER (IF)	OCTS (IF)	Ref. diff. (IF) (%)
1	443	0.1283	0.1338	−4.29
2	490	0.0955	0.0982	−2.83
3	565	0.0599	0.0540	9.85
4	670	0.0318	0.0318	0.00
5	765	0.0185	0.0201	−8.65
6	865	0.0146	0.0158	−8.22

865 nm acquired on 26 April 1997 (pass no. 55; level-1, non-validated). The methods which we consider in this paper are as follows:

1. Method A (A most simple estimation method to minimize the absolute difference between the observed and theoretical values in either reflectance (polarization), or both by assuming refractive index.)
2. Method B (The same as Method A, but without assuming refractive index.)
3. Method C (Estimation method using two channel reflectance data, originally proposed by Stowe et al. [7].)
4. Method D (Estimation method using two channel polarization data, originally proposed by Masuda and Takashima [8].)
5. Method E (Estimation method using both reflectance and polarization data in single channel, proposed by us in this paper.)

As for aerosol size distribution models, we adopted Junge type power law models [6] with the index of $v = 2.5,\ 3.0,\ 3.5,\ 4.0$ and 4.5. In this study we shall use τ_{500} as a measure of the aerosol optical thickness, because the aerosol optical thickness τ_λ at wavelength λ (nm) can be given by Eq. (5) with given τ_{500}:

$$\tau_\lambda = \tau_{500}\left(\frac{\lambda}{500}\right)^{-\alpha}, \tag{5}$$

where α is Ångström exponent and it is related to Junge's index v as follows: $\alpha = v - 2$. Since Ångström exponent is commonly used, we shall use α instead of v, hereafter. In other words, we considered here five different cases of α, namely, $\alpha = 0.5,\ 1.0,\ 1.5,\ 2.0$ and 2.5. The small and large values of α correspond to large and small aerosol particle size cases, respectively. As for aerosol refractive index, we considered six cases of refractive index, i.e., $m = 1.35 - i0.0,\ 1.40 - i0.0,\ 1.45 - i0.0,\ 1.5 - i0.0,\ 1.55 - i0.0$ and $1.60 - i0.0$, where we ignored absorbing aerosol cases. In addition, we used the optical thicknesses of Rayleigh molecules, computed by the formulae in Hansen and Travis's paper [3]. We computed Look Up Tables (LUTs) of the space reflectance and polarization for a given aerosol model with 11 different parameterized aerosol optical thicknesses of τ_{500} from $\tau_{500} = 0.0$ to 1.0 with an increment of

$\Delta\tau_{500} = 0.1$, for 33 different zenith angles of the incident and viewing direction and 72 different azimuthal angles of $\phi - \phi_0$. The LUTs were computed at 670 and 865 nm by the adding and doubling radiative transfer code, including polarization, for 30 aerosol models (5 cases of $\alpha \times 6$ cases of m). In the computation, we assumed a homogeneous atmosphere (mixture of aerosol and Rayleigh particles) bounded by an isotropic Gaussian type ocean surface with a wind speed of $V = 5.0$ m/s. The adoption of such an ocean wind speed is based on the fact that European Center for Medium-Range Weather Forecasts (ECMWF) database indicates the wind speeds for the study scene at near ADEOS observation time in the range of $4.5 < V < 5.7$ (m/s).

Let us define D_r and D_p by Eqs. (6) and (7), respectively:

$$D_r = \frac{1}{2}\left[\frac{1}{n}\sum_{i=1}^{n}\left|R_{obs}^{670}(i) - R_m^{670}(i)\right| + \frac{1}{n}\sum_{i=1}^{n}\left|R_{obs}^{865}(i) - R_m^{865}(i)\right|\right], \tag{6}$$

$$D_p = \frac{1}{2}\left[\frac{1}{n}\sum_{i=1}^{n}\left|P_{obs}^{670}(i) - P_m^{670}(i)\right| + \frac{1}{n}\sum_{i=1}^{n}\left|P_{obs}^{865}(i) - P_m^{865}(i)\right|\right], \tag{7}$$

where n is the total number of viewing directions; i the ith viewing direction; $R_{obs}^{670}(i)$, $R_m^{670}(i)$ and $R_{obs}^{865}(i)$, $R_{obs}^{865}(i)$ are the observed and theoretical space reflectances in the ith direction at 670 and 865 nm; $P_{obs}^{670}(i)$, $P_m^{670}(i)$ and $P_{obs}^{865}(i)$, $P_m^{865}(i)$ are observed and theoretical polarization values in the ith direction at 670 and 865 nm. For the center of each pixel area incident and viewing directions were searched from POLDER's successive scenes and the total number of viewing directions is $n = 12$–14, depending on the pixel area and cloud mask. As for the validation of aerosol optical parameter retrieval, the simultaneous sky observation experiment was made by the skyradiometer (POM-01: PREDE) with six wavelength channels of 315, 400, 500, 870, 940 and 1040 nm at Uchinada Agricultural Experiment Center in Ishikawa Prefecture in Japan, very close to the study site A in Fig. 3. Interpolated aerosol optical thicknesses at 500, 670, and 865 nm were $\tau_{500}[\text{obs}] = 0.2635$, $\tau_{670}[\text{obs}] = 0.1680$, $\tau_{865}[\text{obs}] = 0.1135$, respectively. Ångström exponent deduced from these measurements was $\alpha[\text{obs}] = 1.54$ at ADEOS observation time.

4.1. Results by Method A

We retrieved appropriate aerosol optical parameters (the aerosol optical thickness τ_{500} and Ångström exponent α for each (3×3 pixels) area in the POLDER scene by assuming a fixed m with the aid of the LUTs. In the retrieval scheme, we considered the following algorithm alone: selecting an aerosol model with a set of (τ_{500}, α, m = pre-fixed value) which minimizes

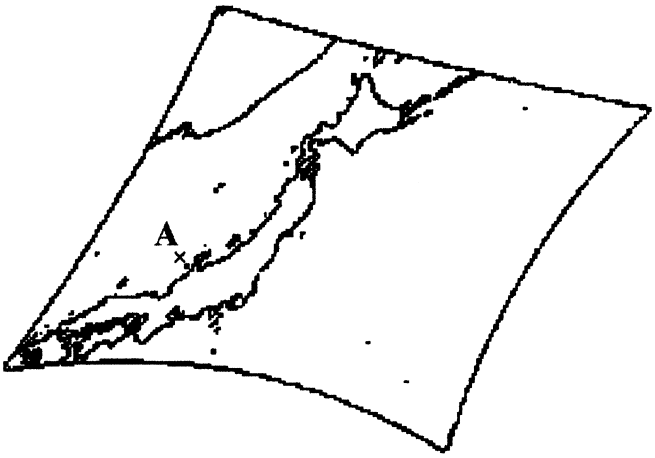

Fig. 3. Location of the study site A, marked by X near the west coast of Japanese main island.

$(D_r + D_p)/2$ among all aerosol models, with the aid of the LUT for each pixel area.

For the case of $m = 1.40 - i0.0$, we present the retrieved distribution maps for τ_{500} and α in Fig. 4(a) and (b), respectively. Fig. 4(a) shows that we have smaller aerosol optical thickness ($\tau_{500} = 0.1$–0.2) in the Pacific Ocean than that ($\tau_{500} = 0.2$–0.5) in the Japan Sea. As for α, we have large regions with $\alpha = 0.5$ (corresponds to large size particles: oceanic particles) in the Pacific Ocean and we have regions with $\alpha = 2.0$ (corresponds to small size particles: land particles) along Japan's main island from Fig. 4(b). The features in Fig. 4 agree generally well with our knowledge about the local atmospheric movement. We have strong Yellow dusts from Asian continent (China) in spring. The retrieved aerosol parameters at the study site A are $\tau_{500} = 0.2$ and $\alpha = 1.0$ and they seem to be underestimated, compared with the measured ones, such as $\tau_{500}[\text{obs}] = 0.2635$, and $\alpha[\text{obs}] = 1.54$. When we assume a different refractive index value, results would be different. In addition, it is difficult to believe that the refractive index of aerosols is constant for all over the area. Therefore, Method A is not recommended for the retrieval. We should note here that we used two viewing directions only with the smallest and largest viewing zenith angles in the retrieval computations by the methods, A and B. This approach using such two viewing directions can be justified by retrieval results using all viewing directions. But they do not show any appreciable difference.

4.2. Results by Method B

This is essentially the same method as Method A, but without assuming fixed refractive index. The following three algorithms were considered here:

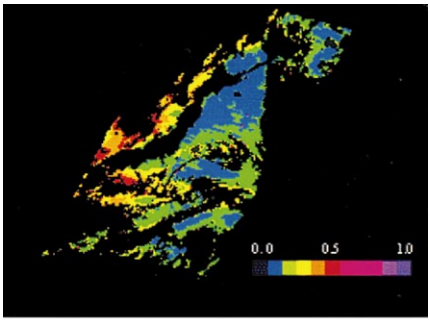

(a)Aerosol Optical Thickness

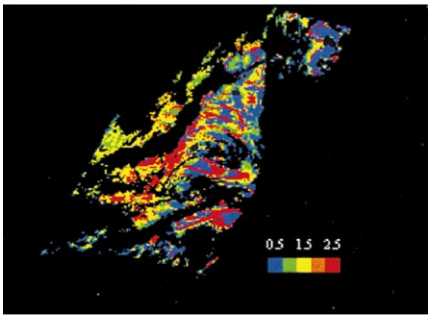

(b)Ångström Exponent

Fig. 4. Retrieved distribution maps from POLDER data on 26 April 1997 by assuming refractive index, $m = 1.40 - i0.0$: (a) aerosol optical thickness at 500 nm; (b) Ångström exponent.

(a) Selecting an aerosol model with a set (τ_{500}, α, m) which minimizes D_r among all aerosol models, with the aid of LUTs for each pixel area.
(b) The same as in (a), except for minimizing D_p.
(c) The same as in (a), except for minimizing $(D_r + D_p)/2$.

We present the retrieved distribution maps (based on algorithm (a)) for τ_{500}, α, and m in Fig. 5(a)–(c), respectively. These are based on space reflectance data alone. The retrieved aerosol parameters at the study site A are $\tau_{500} = 0.2$, $\alpha = 1.5$, $m = 1.55$. The retrieved Ångström exponent is very close to the measured value ($\tau_{500}[\text{obs}] = 1.54$), where as aerosol optical thickness is underestimated, compared with the measured one ($\tau_{500}[\text{obs}] = 0.2633$). The similar distribution maps, based on algorithm (b), are shown in Fig. 6. These results are based on the polarization data alone. We can notice significant changes in all three parameters between Figs. 5 and 6. The retrieval based on the polarization data tends to increase the values of τ_{500} and α significantly. Accordingly, the values of retrieved aerosol

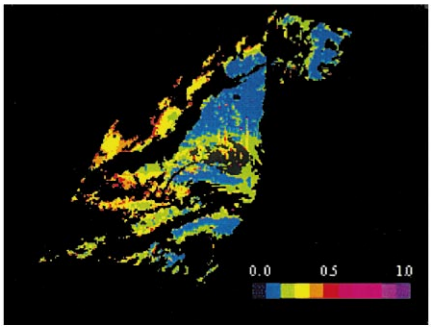

(a)Aerosol Optical Thickness

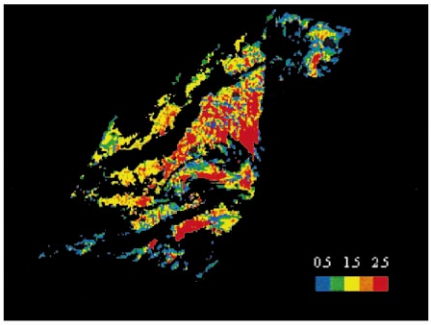

(b)Ångström Exponent

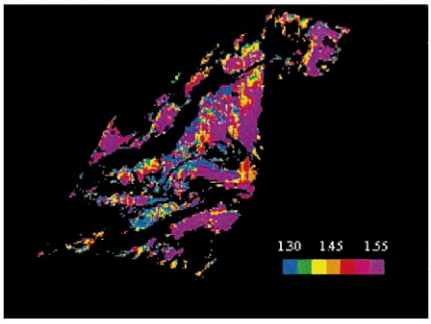

(c)Refractive Index

Fig. 5. Retrieved distribution maps from POLDER's space reflectance data on 26 April 1997: (a) aerosol optical thickness at 500 nm; (b) Ångström exponent; (c) refractive index.

parameters at the study site A increase to a set of $\tau_{500} = 0.3$, $\alpha = 2.0$, and $m = 1.50$. These retrieved values of τ_{500} and α are overestimated, compared with the measured ones, such as $\tau_{500}[\text{obs}] = 0.2635$, and $\alpha[\text{obs}] = 1.54$.

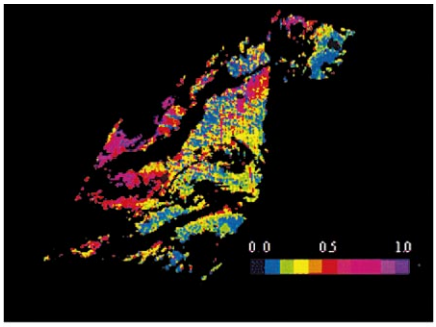

(a)Aerosol Optical Thickness

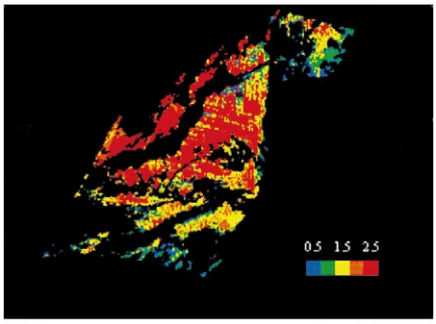

(b)Ångström Exponent

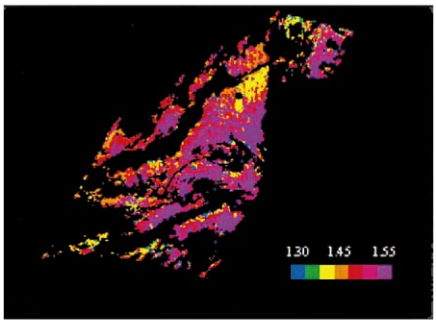

(c)Refractive Index

Fig. 6. The same as in Fig. 5, except from POLDER's polarization data.

Finally, the distribution maps, (based on algorithm (c)) are shown in Fig. 7. These are based on both polarization and space reflectance data. The aerosol optical thickness depends more strongly on the space reflectance than on the polarization, by comparing among Figs. 5(a), 6(a) and 7(a). On

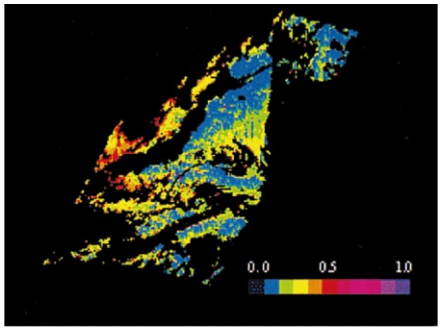

(a)Aerosol Optical Thickness

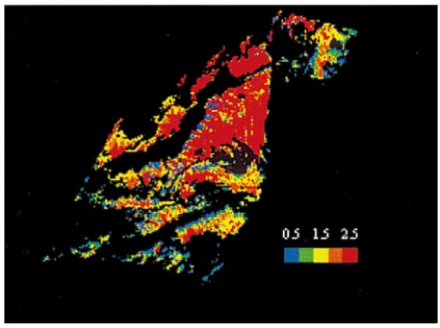

(b)Ångström Exponent

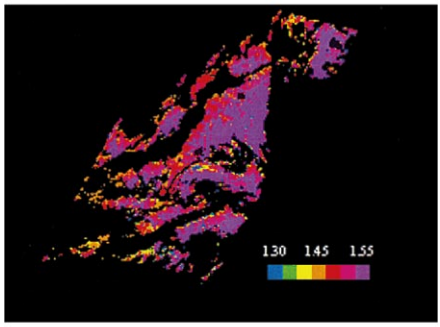

(c)Refractive Index

Fig. 7. The same as in Fig. 5, except from both space reflectance and polarization data of POLDER.

the contrary, the polarization has more influence on distribution patterns of α and m than the space reflectance, since patterns of α and m in Fig. 7(b) and (c) are very similar to those in Fig. 6(b) and (c). The retrieved

parameter values of the study site A are $\tau_{500} = 0.2,\ \alpha = 1.5,\ m = 1.50$, these are very similar to the case of algorithm (a). In the LUT approach, we did not make an interpolation to find the exact values of aerosol optical parameters. In addition, we confirmed that the retrieved results based on the minimum absolute difference between the measured and theoretical values are unstable at some places, because the significant scale difference exists in the space reflectance and polarization unit. Judging from the above limitations, alternative methods by which we can make an interpolation more easily, like Method C–E, seem to give reliable results. We have not completed making aerosol optical parameter maps by Methods C, D, and E. Nevertheless, we present the estimated results by these methods at the study site A and they are described in below.

4.3. Results by Method C

This is a method for estimating aerosol optical parameters, using two channel reflectance values. This method was originally proposed in the retrieval analysis of NOAA/AVHRR data by Stowe et al. [7]. By using a diagram of theoretical space reflectances in 670 and 865 nm channels, parameterized by τ_a and α, for a given angular condition, we can estimate an appropriate set of (τ_a, α) which satisfies the observed space reflectances at 670 and 865 nm. We present the viewing conditions at the study site A in Table 3. Fig. 8(a)–(c) are such space reflectance diagrams at A under the viewing condition of (scene 35: $\theta_0 = 29.14,\ \theta = 55.87,\ \phi - \phi_0 = 88.25$) for $m = 1.35 - i0.0,\ m = 1.40 - i0.0$, and $m = 1.50 - i0.0$, respectively. We can obtain easily three appropriate parameter solutions from a location point (marked by X) with observed space

Table 3
Angular conditions at the study site A in successive scenes from no. 35 to 46, measured by POLDER

Scene no.	θ	$\phi - \phi_0$	θ_0	Θ
35	55.87	88.25	29.14	118.54
36	52.25	93.41	29.09	123.91
37	48.57	99.91	29.05	129.88
38	45.05	108.07	29.01	136.42
39	42.06	118.14	28.96	143.38
40	40.06	130.00	28.92	150.45
41	39.47	142.93	28.88	157.06
42	40.43	155.72	28.83	162.16
43	42.72	167.20	28.79	164.25
44	45.89	176.81	28.75	162.75
45	49.50	184.55	28.70	159.02
46	53.20	190.70	28.66	154.55

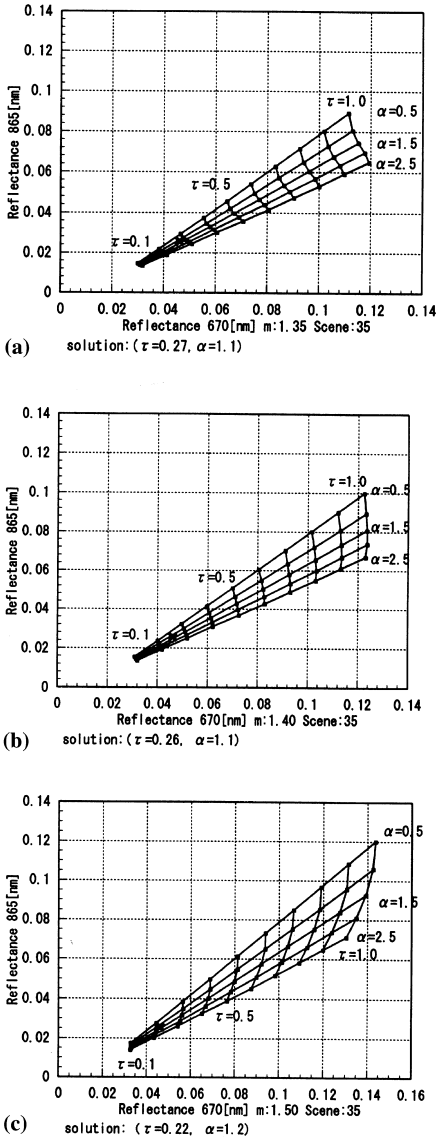

Fig. 8. Two channels space reflectance diagrams under the same angular condition in scene 35: × – location with measured values at the study site A; (a) the case of $m = 1.35 - i0.0$, (b) that of $m = 1.40 - i0.0$, and (c) that of $m = 1.50 - i0.0$.

reflectance values in the diagrams, i.e., $(\tau_{500} = 0.27,\ \alpha = 1.10)$ when $m = 1.35 - i0.0$, $(\tau_{500} = 0.26, \alpha = 1.10)$ when $m = 1.40 - i0.0$, and $(\tau_{500} = 0.22,\ \alpha = 1.20)$ when $m = 1.50 - i0.0$.

4.4. Results by Method D

This is essentially the same method as Method C, except for using two channel polarization values. This method was originally proposed in the analysis of sky polarization data by Masuda and Takashima [8]. The detail analysed results based on the different aerosol size distribution model are given by Masuda et al. [9] in the same issue. The theoretical polarization diagrams are similarily plotted in Fig. 9(a)–(c) for $m = 1.35 - i0.0$, $m = 1.40 - i0.0$, and $m = 1.50 - i0.0$, respectively. We can also obtain three appropriate parameter solutions from diagrams in Fig. 9, i.e., $(\tau_{500} = 0.41, \alpha = 1.37)$ when $m = 1.35 - i0.0$, $(\tau_{500} = 0.36, \alpha = 1.20)$ when $m = 1.40 - i0.0$, and $(\tau_{500} = 0.34, \alpha = 0.80)$ when $m = 1.50 - i0.0$. These results by Method D are very much different from those found by Method C. Again, the estimated value of τ_{500} derived from the polarization data tends to be larger than that derived from the space reflectance data. The different results by both Methods C and D suggest strongly that the parameter estimation should be made by using the space reflectance and polarization information simultaneously.

4.5. Results by Method E

This is our proposed single channel method, using a P–SR (polarization–space reflectance) diagram. By this method, we cannot only solve the above mentioned contradiction, but also make a discrimination of refractive index value. We show three theoretical P–SP diagrams in 865 nm under the same viewing condition in scene 35 for $m = 1.35 - i0.0$, $m = 1.40 - i0.0$, and $m = 1.50 - i0.0$ in Fig. 10(a), (b) and (c), respectively. From the diagrams in Fig. 10, we find easily three appropriate solutions, i.e. $(\tau_{500} = 0.29,\ \alpha = 1.35)$ when $m = 1.35 - i0.0$ $(\tau_{500} = 0.26,\ \alpha = 1.61)$ when $m = 1.40 - i0.0$, and $(\tau_{500_a} = 0.26,\ \alpha = 2.00)$ when $m = 1.50 - i0.0$. Another three diagrams in Fig. 11 are made at the study site A under different viewing conditions of (scene 39: $\theta_0 = 28.96,\ \theta = 42.06,\ \phi - \phi_0 = 118.14$). In this case, we have only one solution of $(\tau_{500} = 0.28,\ \alpha = 1.83)$ when $m = 1.40 - i0.0$. No solution exists when $m = 1.35 - i0.0$ and $m = 1.50 - i0.0$, because X is outside of the parameter diagram in both $m = 1.35 - i0.0$ and $m = 1.50 - i0.0$ cases. We can, therefore, reject the cases of $m = 1.35 - i0.0$ and $m = 1.50 - i0.0$ by including additional viewing conditions. As an appropriate aerosol parameters at the study site A, we find a parameter set of $(\tau_{500} = 0.27,\ \alpha = 1.72,\ m = 1.40 - i0.0)$ by taking an average of two results found in two viewing directions. These values are in good agreement with the measured ones $(\tau_{500}[\text{obs}] = 0.2635,\ \alpha[\text{obs}] = 1.54)$. We should point out here that the simultaneous consideration on both space reflectance and polarization is essential in the retrieval algorithm. From this point of view, our Method E

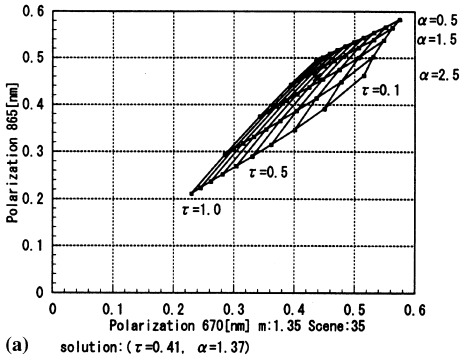

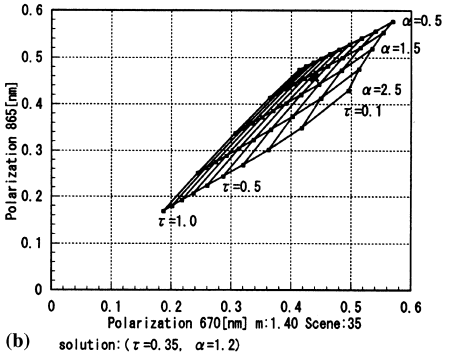

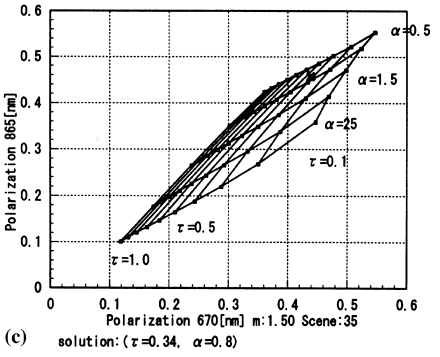

Fig. 9. Two channels polarization diagrams under the same angular condition in scene 35: × – location with measured values at the study site A; (a) the case of $m = 1.35 - i0.0$, (b) that of $m = 1.40 - i0.0$, and (c) that of $m = 1.50 - i0.0$.

seems to be one of the best candidates for retrieving aerosol optical parameters. The implementation of Method E in computer code will come very soon by us.

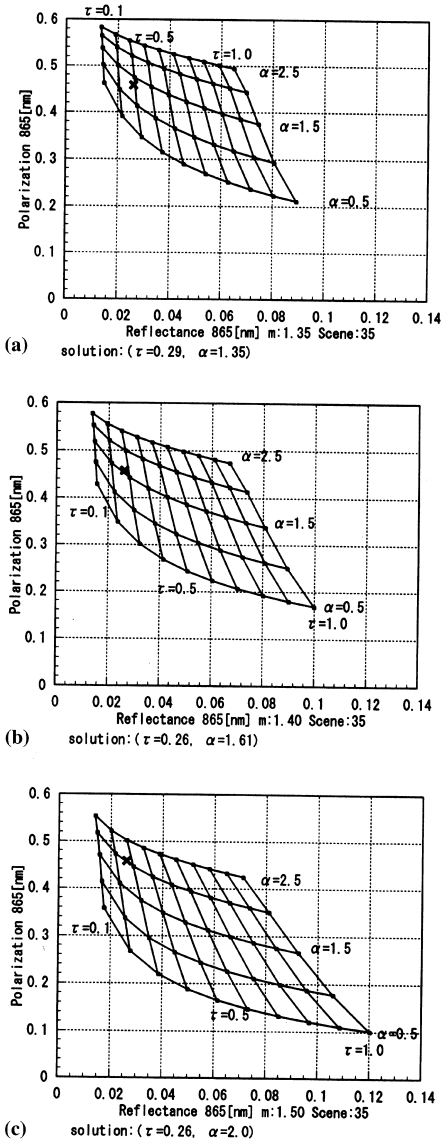

Fig. 10. P–SR diagrams in 865 nm under the same angular condition in scene 35: × – location with measured values at the study site A; (a) the case of $m = 1.35 - i0.0$, (b) that of $m = 1.40 - i0.0$, and (c) that of $m = 1.50 - i0.0$.

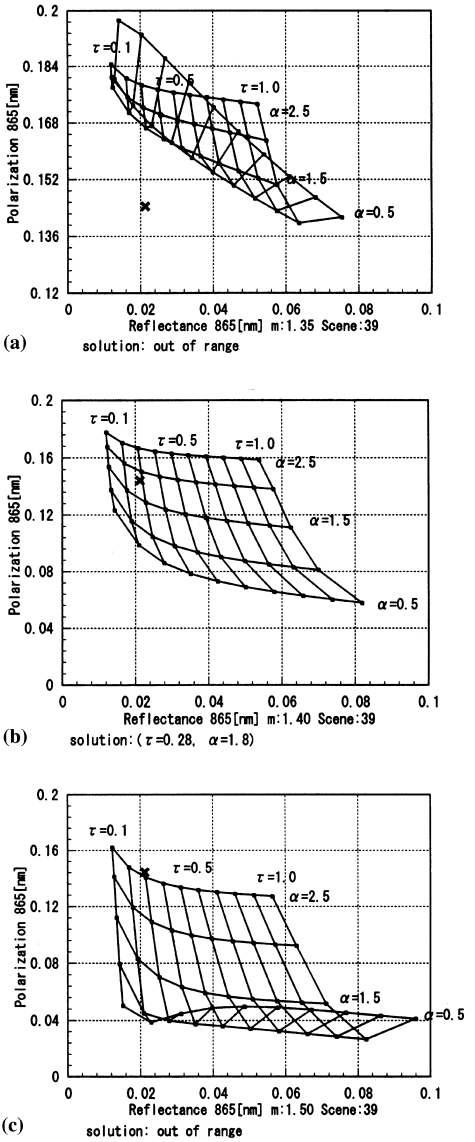

Fig. 11. The same P–SR diagrams, except under the same angular condition in scene 39.

5. Conclusions

Conclusions of this study can be summarized as follows:

1. We made cross calibration between POLDER and OCTS sensors on board ADEOS satellite, by comparing space reflectances of the same ocean target

from two sensors' data acquired simultaneously on 26 April 1997. We found that the in-flight calibration gain factors for both POLDER and OCTS are in good agreement with relative differences of less than 10% in all bands.
2. Then, we retrieved the local aerosol's optical parameters over the Japan Sea and the Pacific Ocean from ADEOS/POLDER's directional reflectance and polarization data, by several retrieval algorithms. The resulting distribution maps for aerosol optical parameters were also presented.
3. We pointed out that the simultaneous consideration on both space reflectance and polarization is essential in the retrieval algorithm. Otherwise, there is a strong possibility that the results by using either reflectance or polarization data are misleading.
4. We proposed a new and good method for retrieving aerosol optical parameters, based on parameterized P–SR diagram. The validity of this method was demonstrated by using simultaneously measured sky observation data.
5. The implementation of our proposed method in computer code is left as our future work.

Acknowledgements

We thank Prof. S. Mukai, and Dr. I. Sano at Kink University very much for their kind help in obtaining OCTS data, and Drs. Masuda and Takashima at MRI for helpful discussions. This study is supported by NASDA Research Contract, NASDA-PSPC-21409. The results were obtained from CNES's POLDER and NASDA's OCTS on board NASDA's ADEOS.

References

[1] O. Hagolle, POLDER in-flight absolute calibration, in: Proceedings of the ALPS'99 by CNES, Meribel, France, WK2-P-11, 18–22 January 1999, pp. 1–4.
[2] Y. Mitomi, M. Toratani et al., Evaluation of OCTS standard ocean color products: comparison between satellite-derived and ship measured values, in: Proceedings of the PORSEC'98, Qingdao, China, 28–31 July 1998, pp. 115–118.
[3] J.E. Hansen, L.D. Travis, Light scattering in planetary atmospheres, Space Sci. Rev. 13 (1974) 527–610.
[4] C. Cox, W. Munk, Measurement of the roughness of the sea surface from photographs of the sun's glitter, J. Opt. Soc. Amer. 44 (11) (1954) 838–850.
[5] Y. Kawata, A. Yamazaki, Multiple scattering analysis of airborne POLDER image data over the sea, IEEE Trans. GRS 36 (1) (1998) 51–60.
[6] T. Junge, Aerosols, in: Campen et al. (Eds.), Handbook of Geophysics, Macmillan, New York, 1960.
[7] L.L. Stowe, A.M. Ignatov, R.R. Singh, Development, validation, and potential enhancements to the second-generation operational aerosol product at the National Environmental Satellite, Data and information service of the national oceanic and atmospheric administration, J. Geophys. Res. 102 (D14) (1997) 16,923–16,934.

[8] K. Masuda, T. Takashima, Retrieval of the optical thickness and Angstrom coefficient of the aerosols over the ocean from polarization measurements by POLDER on board ADEOS satellite, J. Remote Sensing Soc. Jpn. (1999), to appear.
[9] K. Masuda, T. Takashima, Y. Kawata, A. Yamazaki, M. Sasaki, Retrieval of aerosol optical properties over the ocean using multispectral polarization measurements from space, Appl. Math. Comput. 116 (2000) 103–114, in this issue.